

Numerical Analysis of Solar Energy Storage within a Lobed Triplex Tube Heat Exchanger Utilizing Porous Metal Foam and Y-Shaped Fins

Abolfazl NematpourKeshteli¹, Marcello Iasiello¹, Giuseppe Langella¹, Nicola Bianco¹

¹ Dipartimento di Ingegneria Industriale/Università degli Studi di Napoli Federico II
P.le Tecchio 80, 80125, Napoli, Italy
abolfazl.nematpourkeshteli@unina.it

Abstract - Latent heat storage units (LHSU) greatly minimize the issue of solar energy intermittent and discontinuous supply since they allow to storage of large amounts of thermal energy without any temperature gradients. In this category, the most popular solar thermal application of a latent thermal energy storage system (TES), often equipped with Phase Change Material (PCM), is the triplex tube heat exchanger (TTHX). Also, increasing thermal conductivity is a crucial subject to improving storage capacity due to the poor thermal conductivity of PCMs. To improve augmenting the conductivity of paraffin (RT54HC), optimization of the heat exchanger geometry (lobed heat exchanger), using extended surface (Y-shaped fin), and porous metal foams (aluminium foam-20 PPIs and 0.88 porosity) have been used as thermal conductivity enhancers of PCM-based energy storage devices. Heat transfer fluid (H₂O) across inner and outer tubes is considered too as the working fluid. The main goal of this investigation is to develop a highly efficient TES system in domestic and industrial hot water heating applications with a TTHX equipped with the aforementioned thermal conductivity enhancement techniques. To model the PCM melting, an enthalpy-porosity approach is employed, where governing equations are numerically solved with a finite volume approach. When the porous foam is included, a two-energy equation local thermal non-equilibrium model is employed. The findings are summarized in terms of the liquid fraction, temperature evolution, and rate of energy storage charge. The outcomes illustrate that Case B and Case C-pure PCM compared to Case A decreases the charging time by 14.91% and 30.54%, respectively. Also, the addition of metal foam in the lobed pipe (case B) reduces melting time by 73.61% and increases the rate of energy storage when compared to Case A-pure PCM.

Keywords: Heat storage, Concentrated solar unit, Paraffin, Porous metal foam, Finned surfaces, Domestic hot water

1. Introduction

Renewable energy applications in buildings will have a significant influence on future energy savings as construction technology advances. Solar energy is widely used in all industries and has the advantages of infinite storage capacity, non-pollution, and simplicity of access. A crucial technological solution to minimize energy use and a fundamental to improving the energy flexibility of buildings is the integration of solar thermal storage systems with buildings. Thermal Energy Storage (TES) is an important component of solar home hot water systems because it compensates for the temporal mismatch between available solar radiation and hot water demand. Latent Heat Energy Storage (LHES) system utilizes Phase Change Materials (PCMs) to store/release energy in the form of latent heat of fusion, resulting in a higher energy storage density than water-only systems. PCMs also regulate the system temperature to maintain it around the melting point. Because of the low thermal conductivity, the heat transfer rate to the PCMs is slowed, limiting the system's storage capacity for a given charging and discharging duration. Thermal conductivity enhancers such as porous metal foams and geometry modification have been extensively used to improve the self-insulating behaviours of PCM-based energy storage devices.

An experimental TES system using a Triplex Tube Heat Exchanger (TTHX) with fins containing PCM was researched, constructed, tested, and assessed by Abdulateef et al. [1]. They discovered that the rectangular fins outperform the triangular fins by 15%. Yu et al. [2] discovered in their study that using tree-shaped fins leads to a 26.7% decrease in melting time and a 45.4% increase in heat storage rate compared to using conventional fins. Abidi et al. [3] investigated the impact of longitudinal fin design on charging time reduction in a TTHX-LHS system. They demonstrated that melting time would decrease by 34.7% in the best-case scenario. Najafabadi [4] investigated a novel heat storage method for solar collectors using PCM in a twisted double-pipe heat exchanger (DPHX) with a lobed pipe. They proved that the three-lobed DPHX has the maximum heat transfer surface and melts 6% faster than the simple circle cross-section DPHX. Lafdi et al. [5]

investigated the impact of aluminium foam pore size and porosity on PCM melting development. They observed that foams with increased porosity and bigger pore diameters attain steady-state temperatures faster. Mahdi and Nsofor [6] studied a 2D DPHX-LHS system constructed of changing porosity multi-segment metal foam. They found that employing foam with varying porosities in discrete segments improved heat storage and recovery rates over having a single porosity. Iasiello et al. [7] recorded numerical and experimental findings on PCMs with aluminium metal foams under various orientations, porosities, PPIs, and heat fluxes. They reported that the lower the porosity the higher the melting fraction, while PPIs and orientation have no relevant effects on melting time.

According to the studies described here, updating LHTES-TTHX systems can be done in a number of ways. In order to analyse some solutions to improve the thermal performances of PCMs for TTHX, for the first time, a numerical investigation of thermal performances enhancement techniques, that include optimizing the contact surface between the working hot fluid and PCM domain, metal foams, and extended surface, will be carried out here. Paraffin waxes, namely RT54HC, are embedded within aluminium foams with 20 PPIs, and 0.88 porosity. The main concern of this work is to provide which would be the best solution among different ones in order to minimize aspects like melting time and maximize velocity, as well as stored energy. The results will be displayed in terms of liquid fractions, the temperature achieved, the effect of additive metal foam, optimized geometry of the heat exchanger, and fin on the time of complete charging processes and the rate of energy storage. The main features and novelties of the proposed model are resumed in the following: 1) Improving the heat exchanger geometry (lobed heat exchanger); 2) Adding metal foam (aluminium foam); 3) Using extended surface (Y-shaped fin).

2. Incorporation of the solar system with TTHX

One of the most cost-effective methods to have a water heater is to use solar collectors. However, one should theoretically design an appropriate TES system in order to guarantee that hot water is always available at all times by following continuous full charge/discharge cycles. The geometry of the TTHX-TES system used in this application is also shown in cross-section in Figure 1 for three cases: simple TTHX (Case A), lobed TTHX (Case B), and lobed TTHX with a Y-shaped fin (Case C). Water as the working fluid comes from the top-right of the channel, which corresponds to $z = 0$, exiting at the down-left at $z = L$ after heat transfer with the PCM, which changes phase due to heat transfer. The hot inlet fluids from the concentrating solar system flow within the inner and outer tubes, and the middle pipe is surrounded by the PCM and/or porous metal.

3. Assumption and mathematical formulation

The enthalpy-porosity technique was used to anticipate the transient process, with assumptions for the current investigation resumed in Fig 2.

Continuity, momentum and energy equations for both phases, namely PCM and metal foam, are required; these are written below in a porous media volume-averaged generic form, i.e., by assuming that such equations are written over a representative elementary volume of the domain. The phase change process was numerically calculated using the enthalpy-porosity method with the assumption that the porosity and liquid fraction in each cell were identical. Because of the fluid velocity range in the domain, the buoyancy forces generated the Newtonian free convection flow of melted PCM, which was transitory and positioned in the laminar flow regime. The momentum equation also employed the Boussinesq approximation due to the minimal temperature gradient. As a result, the governing equations were developed based on these assumptions and are as follows, with viscous dissipation ignored.

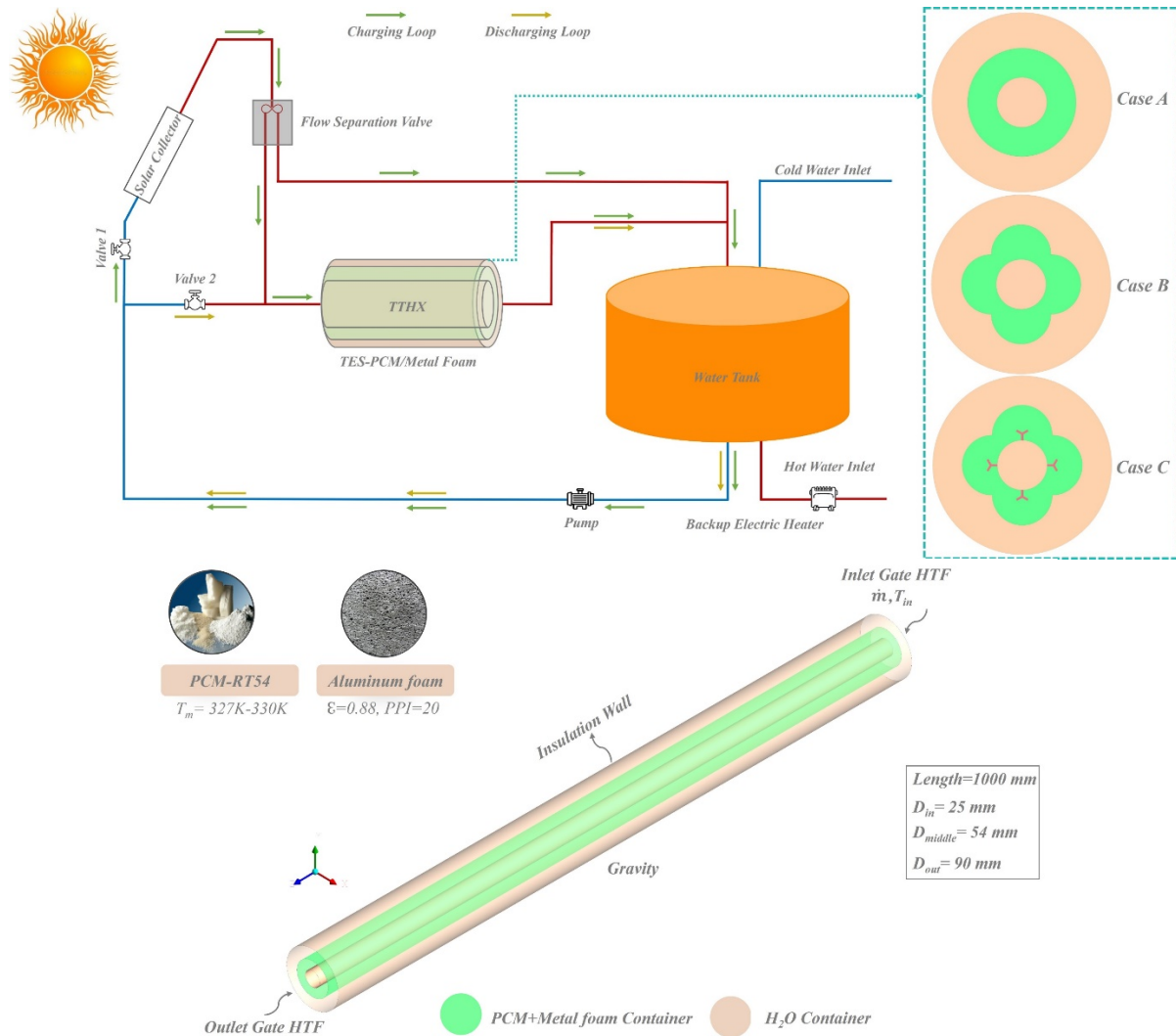


Fig. 1: Configuration of heat storage and solar thermal collector, schematic figure of different cases (A-C) for TTHX, and 3D view of the TTHX.

Assumptions

- (1) Water fluid flow is 3D, steady, Newtonian, laminar, and incompressible;
- (2) Volume expansion of PCM and thermal resistances in the tube metal thickness are negligible;
- (3) Thermophysical properties for PCM too are assumed to be constant in the buoyancy force except for density;
- (4) The outer shell is insulated, then heat transfer with the environment is not considered;
- (5) Boussinesq approximation is used for natural convection in the liquid PCM;
- (6) Structure of porous medium is presumed to be homogeneous, isotropic, and open-celled between porous medium and PCM;
- (7) No heat loss or gain from the surroundings;
- (8) Thermal dispersion in the porous foam can be neglected;
- (9) Time scales are as small as to consider constant boundary conditions;

Fig. 2: Assumptions for the present study.

Continuity:

$$\nabla \cdot \vec{V} = 0 \quad (1)$$

Momentum in x, y and z-directions:

$$\frac{\bar{\rho}}{\varepsilon^2} \left(\varepsilon \frac{\partial u}{\partial t} + V \cdot \nabla u \right) = -\nabla P + \frac{\bar{\mu}}{\varepsilon} \nabla^2 u + \vec{S}_u - \frac{\bar{\mu}}{K} u \quad (2)$$

$$\frac{\bar{\rho}}{\varepsilon^2} \left(\varepsilon \frac{\partial v}{\partial t} + V \cdot \nabla v \right) = -\nabla P + \frac{\bar{\mu}}{\varepsilon} \nabla^2 v + (\overline{\rho\beta}) g(T - T_{ini}) + \vec{S}_v - \frac{\bar{\mu}}{K} v \quad (3)$$

$$\frac{\bar{\rho}}{\varepsilon^2} \left(\varepsilon \frac{\partial w}{\partial t} + V \cdot \nabla w \right) = -\nabla P + \frac{\bar{\mu}}{\varepsilon} \nabla^2 w + \vec{S}_w - \frac{\bar{\mu}}{K} w \quad (4)$$

Energy-PCM and Energy-Porous medium (foam):

$$\overline{\rho c} \left(\varepsilon \frac{\partial T}{\partial t} \right) = k_{fe} \nabla^2 T_f + h_{sf} A_{sf} (T_s - T_f) - \varepsilon \overline{\rho L_f} \frac{\partial \lambda}{\partial t} - \overline{\rho c} (\vec{V} \cdot \nabla T) \quad (5)$$

$$(\rho c)_s \frac{\partial T_s}{\partial t} = k_{se} \nabla^2 T_s - h_{sf} A_{sf} (T_s - T_f) + \varepsilon (\rho c)_s \frac{\partial T_s}{\partial t} \quad (6)$$

Subscripts s and f generally refer to porous medium (foam solid phase) and liquid PCM, respectively. For the HTF, one assumes porosity $\varepsilon = 1$ and $K = \infty$ for the momentum equations. The function ψ is the PCM liquid fraction that ranges in between 0 and 1, defined as:

$$\psi = \begin{cases} 0 & \text{if } T \leq T_s \\ \left(\frac{T - T_s}{T_l - T_s} \right) & \text{if } T_s < T < T_l \\ 1 & \text{if } T \geq T_l \end{cases} \quad (7)$$

Ligament diameter (d_l), pore size (d_p), and porous media closure coefficients for momentum equations are listed as follow [8]:

$$\frac{d_l}{d_p} = 1.18 \sqrt{\frac{1 - \varepsilon}{3\pi} \left(\frac{1}{1 - e^{-\frac{1-\varepsilon}{0.04}}} \right)}, \text{ where } d_p = \frac{0.0254}{\omega}, \omega = 20 \text{ PPI}, \frac{K}{d_p^2} \quad (8)$$

$$= 0.00073(1 - \varepsilon)^{-0.224} \left(\frac{d_l}{d_p} \right)^{-1.11}, \varepsilon = 0.88$$

The Boomsma and Poulikakos model [8] was utilized to calculate the effective thermal conductivity of both PCM (k_{fe}) and the porous medium (k_{se}). Eqs. (5) and (6) also specify the specific surface area and interfacial heat transfer coefficient of metal foams, represented by A_{sf} and h_{sf} respectively.

$$A_{sf} = \frac{3\pi d_l}{(0.59 d_i)^2} \left(1 - e^{-\frac{1-\varepsilon}{0.04}} \right), h_{sf} = \begin{cases} 0.76 Re_d^{0.4} P r_{PCM}^{0.37} \frac{k_f}{d_f}, 1 \leq Re_d \leq 40 \\ 0.52 Re_d^{0.5} P r_{PCM}^{0.37} \frac{k_f}{d_f}, 40 \leq Re_d \leq 1000 \\ 0.26 Re_d^{0.6} P r_{PCM}^{0.37} \frac{k_f}{d_f}, 1000 \leq Re_d \leq 2 \times 10^5 \end{cases} \quad (9)$$

Melting (p_L) heat transfer rate represents the thermal energy stored capacity per unit charging time, which is an average heat rate as a representation of the mean melting velocity and is defined as the stored thermal energy throughout the charging time as follow [9, 10]:

$$p_L = \frac{Q}{t_m} = \frac{m_{pcm} \left(\int_{T_i}^{T_s} c \, dT + L_f + \int_{T_l}^{T_e} c \, dT \right)}{t_m} = \frac{m_{pcm} [c(T_s - T_i) + L_f + c(T_e - T_l)]}{t_m} \quad (10)$$

$$c = 2 \text{ kJ/kg K}, T_s = 327 \text{ K}, T_i = 303 \text{ K}, L_f = 189 \text{ kJ/kg}, T_e = 333 \text{ K}, T_l = 330 \text{ K}$$

4. Numerical solution

4.1. Numerical approach

The unsteady equations stated above have been solved using ANSYS FLUENT 2021R1. For numerical modelling purposes, a 3D domain has been presented, and the finite volume methods (FVM) was used to solve the equations. Simulations based on the FVM were done for both zones, water, and PCM in the laminar regime. Figure 3 depicts brief explanations of the modelling setup and solution strategies that were used.

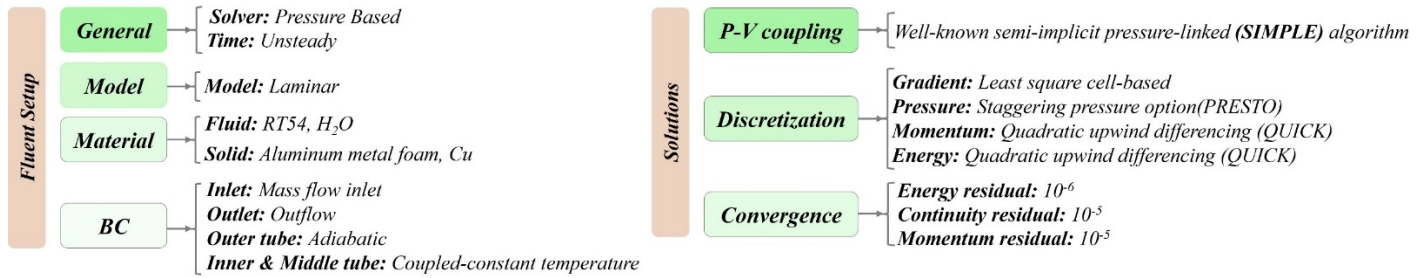


Fig. 3: Summary of selected setup and solution techniques in simulations.

4.2. Validation

The current mathematical model was compared to experimental and computational findings obtained by Al-Abidi et al. [3]. They investigated melting paraffin as PCM (RT82) in a TTHX system. The average temperature profile for PCM during melting for the two experiments and numerical is shown in Figure 4, showing a good agreement. Figure 5 reports comparisons with a nano PCM-metal foam system from Mahdi and Nsofor [11] in terms of the development of the liquid fraction for two distinct porosities (0.95 and 0.98), demonstrating good agreement in this area as well.

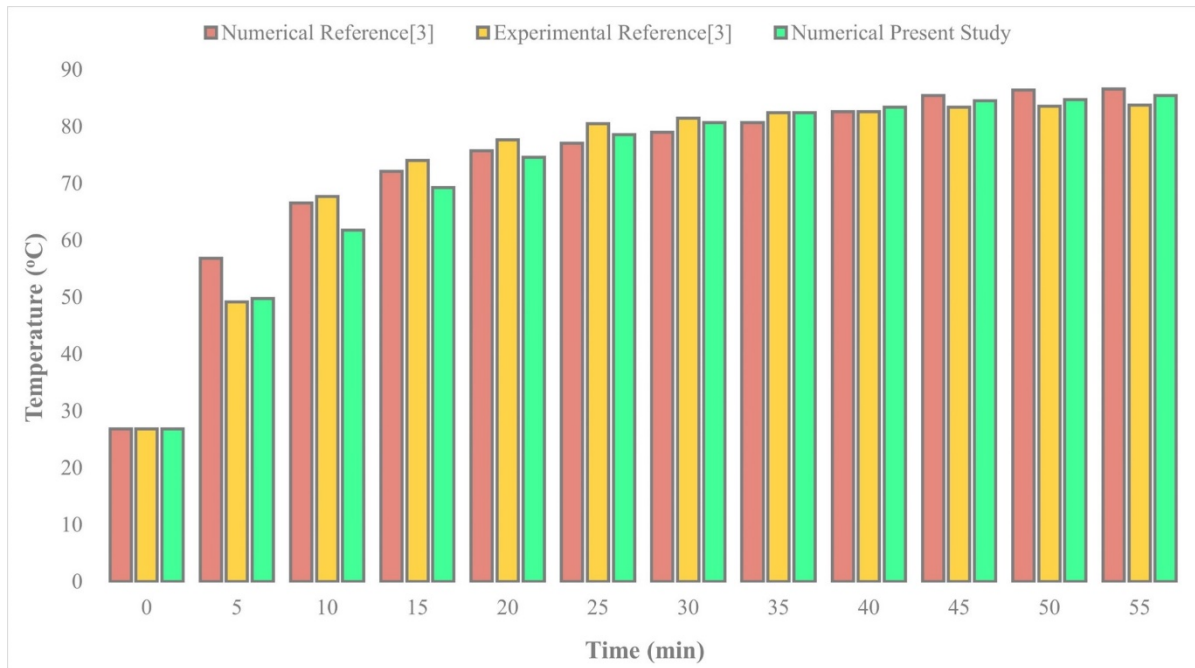


Fig. 4: PCM-averaged temperature vs time: comparisons with experiments and simulations from Al-Abidi et al. [3].

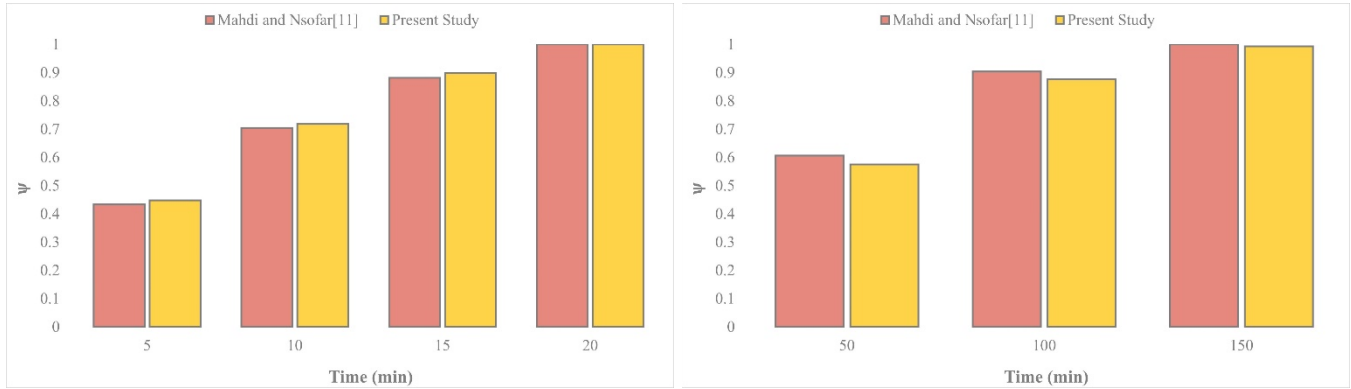


Fig. 5: LF evolution vs time for (left) $\epsilon = 0.95$ and (right) $\epsilon = 0.98$ compared with Mahdi and Nsofar [11].

5. Results and discussion

Comparisons in terms of melting time (t_m), time-saving percentage (%), heat transfer rate (p_L), and contour plots of the liquid fraction and thermal field for all cases with pure PCM (PP) and PCM with metal foam (PP-MF) are shown in Fig. 6. Heat transfer performances in terms of both melting time and heat storage rate look to be far better if optimizing geometry (lobed heat exchanger) and using extended surface (Y-shaped fin) are employed, which means far more PCM is melted at an equal time by adding the aforementioned enhancement methods. The heat transfer rate, for Case B-PP and Case C-PP, is higher than for Case A-PP. This makes melting velocity to be much higher if combined solutions are considered. When comparing Case B-PP, and Case C-PP with pure PCM to Case A-PP with pure PCM, a reduction of 14.91% and 30.54%, respectively in terms of melting time has been found. According to Fig. 6, by comparing lobed pipe and Y-shaped fin with metal foam, the metal foam has a higher impact on melting fractions (73.61%), since it drastically improves local surface area and effective thermal conductivity, with an impact larger than that of the fin.



Fig. 6: A comparison between all cases with PP and metal foam: melting time, time saving and heat transfer rate

As shown in Fig. 7 under the same conditions (mass of PCM), with adding the lobed pipe, the melting process speeds up. This occurs because, when the geometry of the inner tube's cross-section is changed from Case A to Case B, the vortex in the PCM rises, resulting in greater heat transfer and a shorter melting time, also due to the increased heat transfer area. Additionally, it is discovered that the finned model (Case C) performance is superior than Case A because the inclusion of a finned surface enhances the TTHX contact surface with the PCM in both the top and bottom parts, improving the TTHX

temperature distribution. This is because the fins, which also have some natural convection effects, make the top of the TTHX melt quicker. According to Fig. 7, the highest amount of PCM is melted by considering Case B-MF. It is evident from the figures that melting is faster in this case compared to the other ones, especially with references to the Case A-PP, Case B-PP, and also to Case C-PP. This means that employing aluminium foams flavoured with paraffin helps heat transfer, increasing the melting velocity.

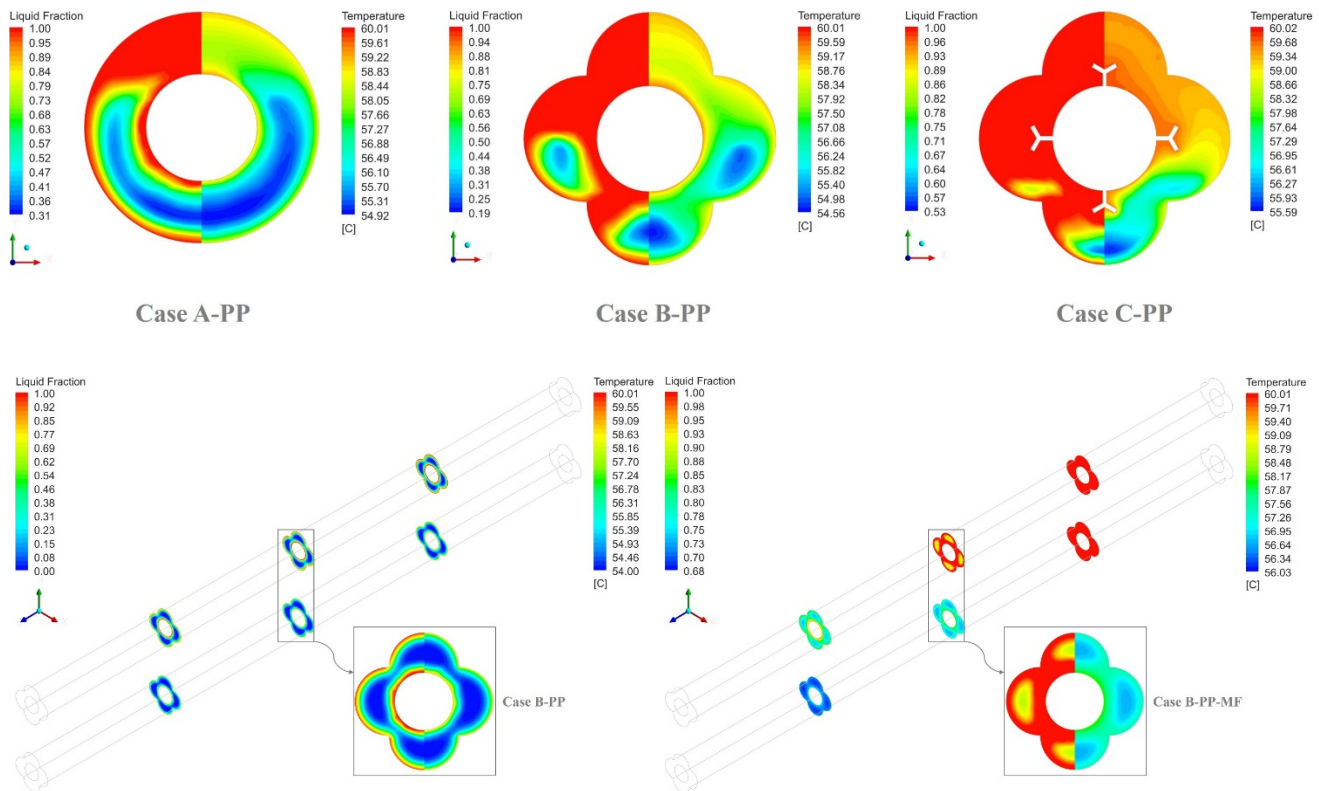


Fig. 7: LF and average temperature contours for (top) cases with PP at $z=L$ cross-sections and $t=1$ hour, (bottom) Case B-PP and Case B-PP-MF at different cross-sections and $t=20$ minutes

6. Conclusion

In this work, Triplex Tube heat exchangers (TTHX) with the incorporation of the solar system that can store energy to provide hot water have been proposed to increase the rate of charging in thermal storage units. TTHX will continue to play an important role in the household and industrial water heating systems system markets. This paper presents numerical predictions that have been performed via a 3D model along with different thermal enhancement solutions for a PCM (RT54HC) in TTHX have been compared. In this study, in order to improve system performance, the effect of optimizing geometry (lobed heat exchanger), using extended surfaces (Y-shaped fin), and porous metal foam (aluminium) with $PPI=20$ and porosity=0.88 are employed. The objective of the present study is to have a throughout comparison of all these solutions to appreciate which one could be the best for thermal energy storage and melting fraction evolution referred to as a TTHX thermal energy storage system. The main conclusions from the present work are listed as follows:

- By optimizing the heat exchanger geometry (lobed heat exchanger), and using lobed pipes with Y-shaped fin, melting times were significantly reduced, so that Case B-PP Case C-PP respectively has the best performance compared to Case A-PP in terms of melting time, time saving and rate of heat energy storage.

- With the addition of lobed (Case B) and Y-shaped fin (Case C), in TTHX, the rate of heat energy storage has been 70.77 W and 86.71 W, respectively.
- Compared to TTHX (Case A-PP) without metal foam, adding a lobed with metal foam (Case B-PP-MF) has a substantial influence on lowering melting time (73.61%).
- The addition metal foam to PCM in Case B has resulted in a heat storage rate increase of 228.20 W.

Acknowledgements

This work was supported by Italian Government MIUR Grant No. PRIN-2017F7KZWS

References

- [1] A. M. Abdulateef, S. Mat, K. Sopian, J. Abdulateef, and A. A. Gitan, "Experimental and computational study of melting phase-change material in a triplex tube heat exchanger with longitudinal/triangular fins," *Solar Energy*, vol.155, pp. 142-153, 2017
- [2] C. Yu, S. Wu, Y. Huang, F. Yao and X. Liu, "Charging performance optimization of a latent heat storage unit with fractal tree-like fins," *Journal of Energy Storage*, vol. 30, pp. 101498, 2020.
- [3] A. A. Al-Abidi, S. Mat, K. Sopian, M. Y. Sulaiman, and A. T. Mohammad, "Internal and external fin heat transfer enhancement technique for latent heat thermal energy storage in triplex tube heat exchangers," *Applied thermal engineering*, vol. 53, no. 1, pp. 147-156, 2013.
- [4] M. F. Najafabadi, H. T. Rostami, and M. Farhadi, "Analysis of a twisted double-pipe heat exchanger with lobed cross-section as a novel heat storage unit for solar collectors using phase-change material," *International Communications in Heat and Mass Transfer*, vol. 128, pp. 105598, 2021.
- [5] K. Lafdi, O. Mesalhy, S. Shaikh, "Experimental study on the influence of foam porosity and pore size on the melting of phase change materials," *Journal of Applied Physics*, vol. 102, no. 8, pp. 083549, 2007.
- [6] J. M. Mahdi, and E. C. Nsofor, "Multiple-segment metal foam application in the shell-and-tube PCM thermal energy storage system," *Journal of Energy Storage*, vol. 20, no. 1, pp. 529-41, 2018.
- [7] M. Iasiello, M. Mameli, S. Filippeschi, N. Bianco, "Metal foam/PCM melting evolution analysis: Orientation and morphology effects," *Applied Thermal Engineering*, vol. 187, pp. 116572, 2021.
- [8] K. Boomsma, and D. Poulikakos, "On the effective thermal conductivity of a three-dimensionally structured fluid-saturated metal foam." *International Journal of Heat and Mass Transfer*, vol 44, no. 4, pp. 827-836, 2001.
- [9] H.A. Adine, H. El Qarnia, "Numerical analysis of the thermal behaviour of a shell-and-tube heat storage unit using phase change materials." *Applied mathematical modelling*, vol. 33, n. 4, pp. 2132-44, 2009.
- [10] Y. Xu, Q. Ren, ZJ Zheng, YL He, "Evaluation and optimization of melting performance for a latent heat thermal energy storage unit partially filled with porous media." *Applied energy*, vol. 193, pp. 84-95, 2017.
- [11] J. M. Mahdi, and E. C. Nsofor, "Melting enhancement in triplex-tube latent heat energy storage system using nanoparticles-MF combination." *Applied energy*, vol. 191, PP. 22-34, 2017.